Structure in the Ionization Near Threshold of Rare Gases by Electron Impact*

S. N. Foner and B. H. Nall
Applied Physics Laboratory, The Johns Hopkins University, Silver Spring, Maryland
(Received August 1, 1960; revised manuscript received January 25, 1961)

Ionization efficiency curves for xenon, krypton, and argon have been studied with an electron energy analyzer. The electron energy distribution was measured and the absolute voltage scale determined in each experiment. The results of these studies (1) favor a linear threshold ionization law over a 1.127 power law, and (2) show that the data cannot be explained simply by ionization processes with onsets at the $^2P_{\frac{3}{2}}$ and $^2P_{\frac{1}{2}}$ ground states of the ion, but can be well fitted by a series of linear processes. The ionization potentials obtained by extrapolating according to a linear threshold law agree with spectroscopic values to within 0.02 ev. New onsets in argon were observed at about 0.64 v and 1.27 v above threshold. The observed structures in the rare gases are not readily explained by auto-ionization and no alternative explanation is offered. The structures observed in these experiments are compared with the results obtained by other "high-resolution" techniques. This comparison is complicated by the disparity in the published data on onset energies, and by the even greater disagreement on the relative probabilities for the various ionization processes. An independent check on consistency of data was made by comparison with "low-resolution" data obtained on a conventional mass spectrometer. The present data are in excellent agreement with the lower resolution data, while some of the other "high-resolution" data are not.

I. INTRODUCTION

IONIZATION of atoms by electron impact has been studied experimentally for more than forty years. In particular, ionization near threshold in Hg was studied by Lawrence[1] and later by Nottingham[2] with magnetically analyzed electrons which were characterized by having sharp upper limits to their energies. These electron energy distributions were measured directly. Structures observed by Nottingham in the Hg ionization curve were essentially the same as those observed by Lawrence. Stevenson and Hipple[3] studied the form of the ionization curves for argon and neon and found, in particular, evidence for structure near threshold in the A^+ cross section. However, their electron energy distribution was admittedly not as good as Nottingham's. More recently, Fox *et al.*[4] introduced a new approach to the problem of obtaining monoenergetic electrons, i.e., they used the distribution available from a thermionic emitter but by an ingenious retarding potential difference technique (RPD) attempted to simulate a monoenergetic system. Shortly after these workers published their results on rare gases,[4,5] Clarke[6] reported ionization studies using an electrostatic selector, as did Hutchison.[7]

The RPD method has been widely used by various workers. The results favor rather consistently a linear threshold law for single ionization, yet some of the results show large variations, as for example, in krypton.[5,8,9] Also, the RPD results for double ionization in xenon[10] indicate a linear threshold law in contradiction to the square law observed by Clarke[6] and by Morrison,[11] and predicted by theory.[12,13]

Although the apparently higher resolution of the RPD method has made it more attractive than other systems for obtaining nearly monoenergetic electrons, there are two significant disadvantages to the method: (1) The RPD operation is not strictly amenable to theory, especially with respect to clipping of transverse components of velocity by the narrow slits and to the effects of the magnetic field[14]; (2) the apparently narrow electron energy distribution has been checked only indirectly by deduction from electron impact experiments.[15] On the other hand, operation of both the magnetic field velocity selector[2] and the electrostatic energy selector[16–19] are easily treated theoretically, their performance can be closely predicted, and the electron energy distribution can be checked directly.

Three important reasons can be cited for making direct measurements of the electron energy distribution used in ionization studies: (1) Knowledge of the electron energy distribution is maintained throughout the experiment. (2) The shape of the distribution is important in analyzing the data, i.e., in determining the form of the threshold law. (3) The absolute values for the ionization potential (I.P.) and other onset energies can be determined.

It appeared worthwhile, in spite of the experimental difficulties involved, to undertake ionization threshold studies using an electrostatic energy analyzer because

* This work supported by the Bureau of Naval Weapons, Department of the Navy.

[1] E. O. Lawrence, Phys. Rev. **28**, 947 (1926).
[2] W. B. Nottingham, Phys. Rev. **55**, 203 (1939).
[3] D. P. Stevenson and J. A. Hipple, Phys. Rev. **62**, 237 (1942).
[4] R. E. Fox, W. M. Hickam, T. Kjeldaas, Jr., and D. J. Grove, Phys. Rev. **84**, 859 (1951).
[5] R. E. Fox, W. M. Hickam, and T. Kjeldaas, Jr., Phys. Rev. **89**, 555 (1953).
[6] E. M. Clarke, Can. J. Phys. **32**, 764 (1954).
[7] D. A. Hutchison, J. Chem. Phys. **24**, 628A (1956).
[8] D. C. Frost and C. A. McDowell, Proc. Roy. Soc. (London) **232**, 227 (1955).
[9] J. F. Burns, Ph.D. dissertation, University of Tennessee, 1954 (unpublished).
[10] W. M. Hickam, R. E. Fox, and T. Kjeldaas, Jr., Phys. Rev. **96**, 63 (1954).
[11] J. D. Morrison and A. J. C. Nicholson, J. Chem. Phys. **31**, 1320 (1959).
[12] G. H. Wannier, Phys. Rev. **100**, 1180 (1955).
[13] S. Geltman, Phys. Rev. **102**, 171 (1956).
[14] R. E. Fox, W. M. Hickam, D. J. Grove, and T. Kjeldaas, Jr., Rev. Sci. Instr. **26**, 1101 (1955).
[15] W. M. Hickam and R. E. Fox, J. Chem. Phys. **25**, 642 (1956).
[16] A. Ll. Hughes and V. Rojansky, Phys. Rev. **34**, 284 (1929).
[17] A. Ll. Hughes and J. H. McMillen, Phys. Rev. **34**, 291 (1929).
[18] G. D. Yarnold and H. C. Bolton, J. Sci. Instr. **26**, 38 (1949).
[19] G. A. Harrower, Rev. Sci. Instr. **26**, 850 (1955).

of the more straightforward operation and analysis of this system. The work here was aimed at obtaining threshold ionization data with a very simple apparatus that provided means for direct electron energy measurement. Xenon and krypton were chosen for the first experiments because of their large ionization cross sections, their low I.P.'s, and the potentially-resolvable doublet ground states of the ions. Only after considerable experience had been gained on these atoms was argon, having less favorable characteristics, added.

II. EXPERIMENTAL

Physical Layout

A parallel plate electrostatic energy analyzer[18,19] and a crude form of Pierce electron gun[20] were used in these experiments. The analyzer plate separation was 15.8 mm; the slits were spaced 50 mm apart; the slit openings were about 0.2×6.0 mm. The electron source was a tungsten ribbon filament spaced about 40 mm from the entrance slit.

Figure 1 shows the physical arrangement of the ionization chamber, omitting the electron gun and all of the analyzer except the exit slit. A serves both as an electrostatic shield and as a differential pumping aperture. B serves both as the electron accelerator and as a differential pumping aperture. The ion chamber, C, consists of (1) a grid of parallel wires shown dashed in the figure; (2) an efficient Faraday cage electron collector; (3) an outer shell extending to the left from the Faraday cage to fit concentrically over a portion of B. The ion collector, D, consists of three parallel small-diameter wires placed concentrically around the grid. By using an ion collector of extremely small surface area, photoelectric effects are minimized and the time constant in the collector circuit is kept reasonably short.

All system parts except the electron gun were made of brass. The procedure found effective in assembling a stable electron analyzer was to clean the brass abrasively, insert it into the vacuum system, and, thereafter, to maintain the temperature substantially above ambient.

Vacuum System

The vacuum system has a speed of about 10 liters/sec and an ultimate pressure of approximately 5×10^{-7} mm Hg. The sample flow system has a leak rate of approximately 0.85×10^{-7} liter atm/sec for argon. A sample of argon at 700 mm Hg provides an ion chamber pressure of about 1.8×10^{-4} mm Hg. Sample pressures used here were in the range 100–700 mm Hg.

Ionization gauges measure the pressures in the sample line preceding the ionization chamber and in the main vacuum system. The pressure in the ionization chamber can be calculated from the geometry of the connecting apertures and the ionization gauge readings.

[20] J. R. Pierce, *Theory and Design of Electron Beams* (D. Van Nostrand Company, Inc., Princeton, 1954), p. 174.

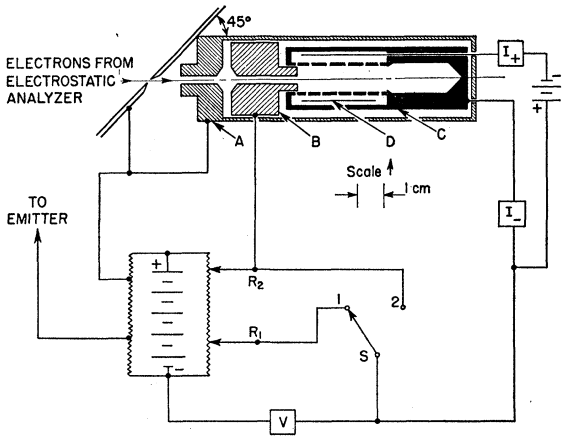

FIG. 1. Ionization chamber and Faraday cage for measuring electron energy distribution. The cross-section view shows the exit slit of the electron energy analyzer and all of the ionization chamber electrodes. A is a shield; B is the electron accelerator; C is the ionization chamber; D is the ion collector; R_1 and R_2 are precision decade voltage dividers. The switch S is in position for a retarding potential analysis of the electron energy distribution. The decade divider R_1 produces known incremental voltage steps of about 0.01 v and the corresponding changes in electron current are measured by the G. R. Electrometer $I-$. A plot of $\Delta I-/\Delta V$ vs V is the electron energy distribution function. The absolute voltage scale is established by taking the voltage V_0 (measured with a precision potentiometer) corresponding to the center of gravity of the electron energy distribution as zero energy. In carrying out ionization experiments, switch S is turned to position 2, placing B and C at the same potential (forming a unipotential ionization chamber). The mean electron energy for a voltage reading V is then given by the difference $V-V_0$, and the ion current corresponding to this energy is measured by the electrometer $I+$.

Field Effects

Helmholz coils are used to neutralize magnetic fields in the vicinity of the analyzer and the ion chamber. A fixed negative voltage between the ion collector and the ion chamber allows collection only of positive ions. The low optical transmission of the grid surrounding the volume where ionization takes place assures adequate shielding of this region from the 3-wire ion collector field. Tests showed that the ion intensity was independent of the ion collector potential over a range of values considerably in excess of those used in these experiments. Because of the approximate 30% transmission factor of the ion chamber grid, the instrument is not ideal for measurements of total ionization cross sections. Measurements were made which indicate that the ions diffuse from the inner region through the grid before experiencing the collector field. For each set of ionization data, the electron energy distribution measurements were made with the same relative potential on the ion collector that exists during ionization. All of the ion chamber, C, becomes a second, larger Faraday cage when the electron energy distribution is measured.

Ion Current Measurements

Ion currents are measured by an inversion-to-ac type electrometer having a sensitivity of about 2×10^{-16} amp. The output of the phase-sensitive detector feeds a Varian 100-mv full-scale recorder. The ion current develops a voltage across the input resistance, which is manually balanced out by a calibrated voltage of opposite polarity. Thus, electrometer operating conditions are maintained constant for all values of the ion current.

Electron Voltage and Current Measurements

Voltage measurements are made with a precision voltage divider and Rubicon potentiometer combination which introduces a maximum error of 0.010 v at 15 v. Electron currents are measured with a General Radio Type 1230-A Electrometer using a 10^9-ohm input resistor. The input impedance is reduced by inverse feedback to about 10^6 ohms, which results in negligible ($\sim3\times10^{-4}$ v) voltage drop across the instrument and thereby, in negligible effect on the measured value of electron energy.

Analyzer Performance

The narrowest electron energy distributions used in obtaining ionization data are about 30–50% greater than predicted purely from dimensional parameters. Less stable operation results if efforts are made to more closely approach the theoretically predicted distributions. Practicable slit shapes, inhomogeneities in analyzer surfaces, and continuous evaporation of oxides and other contaminants from the heated electron source add together to prevent the attainment of the theoretical performance. The continuous evaporation from the filament ultimately degrades the performance of the analyzer to an unsatisfactory state. It has been found that the procedure of dismantling the gun, cleaning it and the first slit, and reassembling the unit without disturbing the analyzer usually restores peak current and good electron energy distribution. Under typical operating conditions, a maximum current of 3×10^{-10} amp through the analyzer is obtained from a total electron emission of 0.01–0.05 ma. The typical spread in energy between the half-maximum points of the distribution is about 0.11 ev. These results are substantially better than those obtained by Fowler and Farnsworth[21] who used a different geometry in their studies of reflection of slow electrons. A narrower distribution from an electrostatic analyzer has recently been reported by Marmet and Kerwin[22] who measured a width at half-maximum of only 0.05 ev. These authors, however, mistakenly concluded that further improvement in resolution would not be very useful because the thermal energy of gas molecules at ordinary source temperatures is of this magnitude. Actually, for ionization of an atom such as argon at 300°K, thermal motion would result in an uncertainty of only about 0.003 ev, which leaves considerable room for improving the instrumentation.

III. IONIZATION NEAR THRESHOLD BY ELECTRONS WITH AN ENERGY SPREAD

In the ideal case of the truly monoenergetic electron beam, a plot of ion current versus the energy of the beam would give directly the form of the ionization threshold law. In practice, the electron energy distribution falls short even of being the triangular distribution expected from the energy analyzer. As a result of the finite width of the distribution, there is threshold curvature which masks the form of the ionization law in the threshold region. If the ionization process continues unchanged from threshold to several electron energy widths above threshold, a simple form of threshold law may still be determined by inspection. Hence, one could expect to distinguish with certainty between a linear and a square threshold law, with less certainty between a linear and a hypothetical $\frac{3}{2}$ power threshold law. When the difference narrows to that between present theories, i.e., between a linear law[13,23] and a 1.127 power threshold law[24] which may hold for only a small energy range above threshold, no choice can be made.

If the electron energy distribution function is known, then, for any particular threshold law the exact shape of the experimental curve can be synthesized, and all ionization data observed in the threshold region are useful in determining which threshold law is applicable. In the usual case, the data exhibit some scatter and this procedure is not sufficient to provide an unambiguous choice between slightly different power laws. Clearly, additional information is needed.

Such additional information is provided by establishing an absolute energy scale for the electrons. It is shown in the following that for certain ionization laws and for reasonably "narrow" electron energy distributions, the extrapolated threshold intercept is equal to the ionization potential.

Electrons leave the electrostatic analyzer with a certain preselected average energy and a distribution about this energy, both of which can be determined by stopping potential measurements. In an ionization experiment, the analyzer operating voltages are constant and the energy of the electrons is varied by changing the potential of the ionization chamber, C (Fig. 1) which is also at the same potential as the electron accelerator, B. The electron energy distribution has a certain functional dependence $f(x)$ which remains

[21] H. A. Fowler and H. E. Farnsworth, Phys. Rev. **111**, 103 (1958).
[22] Paul Marmet and Larkin Kerwin, Can. J. Phys. **38**, 787 (1960).
[24] D. R. Bates, A. Fundaminsky, and H. S. W. Massey, Trans. Roy. Soc. (London) **A243**, 93 (1950).
[24] G. H. Wannier, Phys. Rev. **90**, 817 (1953).

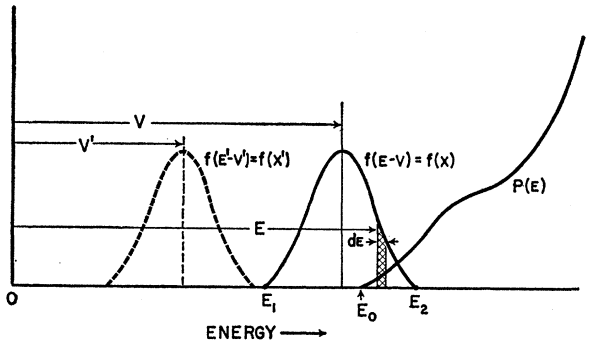

FIG. 2. Ionization by an electron energy distribution. Electrons leave the analyzer with average energy V' and are accelerated into the ionization chamber by the potential V. $P(E)$ is an arbitrary ionization probability function. E_0 is the ionization potential.

unchanged by the acceleration, as is illustrated in Fig. 2. If the electrons leave the analyzer with an average energy V', then acceleration by the potential V simply shifts the entire energy distribution so that the average electron energy becomes V. The ion intensity is proportional to the integral of the product of ionization probability function $P(E)$ and the electron energy distribution function $f(E-V)$. Thus, aside from some numerical proportionality factors such as pressure, electron current, etc., the ion current $I(V)$ is given by

$$I(V)=\int_{E_1}^{E_2} P(E)f(E-V)dE. \tag{1}$$

There are two cases of particular interest for single ionization: the linear threshold law, and the 1.127 power law.

For the linear law, the formulation is quite simple when $E_1>E_0$. The ionization probability is $P(E)=(E-E_0)$ for $E\geq E_0$ and $P(E)=0$ for $E\leq E_0$. The ion current is, then,

$$I(V)=\int_{E_1}^{E_2}(E-E_0)f(E-V)dE = \int_{x_1}^{x_2}(V-E_0+x)f(x)dx,$$

where $x=E-V$. Now

$$\int_{x_1}^{x_2} xf(x)dx=0$$

since the average energy of the distribution is taken as a reference. It follows that

$$I(V)=A(V-E_0) \quad \text{for} \quad E_1>E_0, \tag{2}$$

where

$$A=\int_{x_1}^{x_2} f(x)dx,$$

a constant in an experiment. This straight line, on extrapolation to threshold, gives the correct value of the ionization potential, $V=E_0=$I.P.

In the case of the 1.127 power threshold law, the calculation proceeds in a similar way to give

$$I(V)=\int_{x_1}^{x_2}(V-E_0+x)^{1.127}f(x)dx. \tag{3}$$

Although integration in closed form is straightforward, it is more desirable, in studying the effects of extrapolation, to rewrite the equation in the form

$$I(V)/(V-E_0)^{1.127}=\int_{x_1}^{x_2}[1+x/(V-E_0)]^{1.127}f(x)dx,$$

expand the integrand in a convergent series, and integrate to obtain

$$I(V)/(V-E_0)^{1.127} = A\{1+0.0715B/(V-E_0)^2-0.021C/(V-E_0)^3 +0.0099D/(V-E_0)^4-0.0056E/(V-E_0)^5+\ldots\}, \tag{4}$$

where the constants B, C, D, etc., are the second, third, and fourth, etc., moments of the electron energy distribution function. For symmetrical distributions it can be shown that the observed ion current is $I(V)=A(V-E_0)^{1.127}$ to within a few hundredths of a percent for $(V-E_0)\geq 2(x_2-x_1)$, i.e., two electron distribution widths above onset. Extrapolation of this curve from values of $(V-E_0)>2(x_2-x_1)$ to threshold gives $V=E_0=$I.P. to well within the experimental error for our electron energy distributions.

Extension of this treatment is readily made to higher power threshold laws. For example, the ion current for a quadratic threshold law has the form

$$I(V)=A\{(V-E_0)^2+B\},$$

where A and B are easily determined constants, and extrapolation of the ion current according to this expression from energies more than one electron distribution width above threshold will give the correct ionization potential.

In the transition region, $E_1<E_0$ and $E_2>E_0$, when only a part of the electron distribution is above threshold, the ion current curve exhibits rounding which can be calculated for any particular threshold law if the electron distribution function is known. In these experiments, the electron distribution function is measured and the rounding expected for various threshold laws computed.

IV. IONIZATION DATA AND ANALYSIS

Ionization Near Threshold

Ionization studies have been made for the rare gases with relatively low ionization potentials: xenon, krypton, and argon. In the threshold region, the ion current follows approximately a linear law as opposed

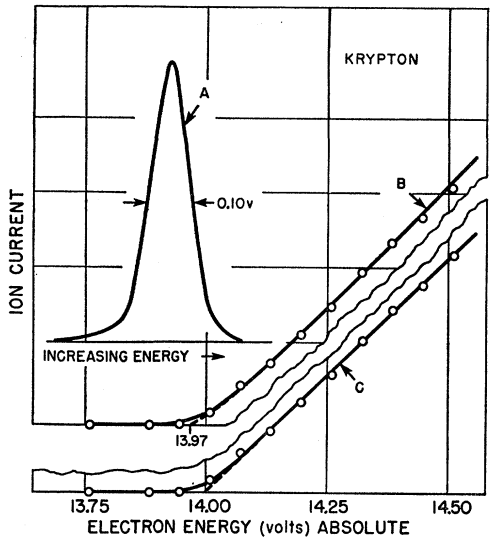

FIG. 3. A test of ionization threshold laws with krypton data. *B* is a synthetic curve obtained by integrating the product of the distribution function *A* and a 1.127 power threshold law. *C* is similar to *B* except that the threshold law is assumed to be linear.

to a higher power law, but the distinction between a linear law and a 1.127 power law is not apparent from inspection of the curves. In order to discriminate between these alternative threshold laws, synthetic curves were constructed for each case by using Eq. (1) with the experimentally measured electron distribution function. The resulting curves were normalized for best fit to the experimental data. Ionization potentials were also obtained for each case and compared with the known spectroscopic energies.

The ionization near threshold for krypton is shown in Fig. 3. Curves *B* and *C* were calculated for a 1.127 power law and a linear law, respectively, using the measured electron energy distribution function *A*. The experimental points are almost equally well fitted by either power law formulation. However, the extrapolated intercept in the case of the linear law, 14.004 ev, is closer to the spectroscopic I.P., 13.999 ev, than the extrapolated intercept for the 1.127 power law, 13.971 ev.

Similar analyses have been made for a series of experiments in xenon, krypton, and argon with the results given in Table I. In xenon and in krypton there is, on the average, a better fit to a linear threshold law. In the case of argon, the occurrence of a new onset close to threshold restricts the number of data points available for analysis and therefore allows the data to be equally well fitted by either law. The average linear threshold law determinations of I.P. in xenon, krypton, and argon deviate from the spectroscopic values by −0.009, +0.013, and −0.020 ev, respectively. The average 1.127 power threshold law determinations deviate by −0.047, −0.020, and −0.039 ev, respec-

TABLE I. Ionization potential determinations, deviations from spectroscopic values,[a] and relative fit of data to threshold laws.

Experiment number	Linear law: Ionization potential (ev)	Linear law: Deviation (ev)	1.127 power law: Ionization potential (ev)	1.127 power law: Deviation (ev)	Half-width of electron energy distribution (ev)	Fit of data favors[b]: Linear law	Fit of data favors[b]: 1.127 power law
			Xenon (Spectroscopic I.P. = 12.129 ev)				
1	12.090	−0.039	12.050	−0.079	0.20+		x
2	12.124	−0.005	12.081	−0.048	0.12+	x	
3	12.144	+0.015	12.109	−0.020	0.12	x	
4	12.121	−0.008	12.090	−0.039	0.10	x	
Average	12.120	−0.009	12.082	−0.047			
			Krypton (Spectroscopic I.P. = 13.999 ev)				
1	13.991	−0.008	13.960	−0.039	0.12	x	
2	13.981	−0.018	13.939	−0.060	0.12+	x	
3	14.051	+0.052	14.026	+0.027	0.15+		x
4	14.047	+0.048	14.007	+0.008	0.17		x
5	13.988	−0.011	13.957	−0.042	0.13+	x	
6	14.013	+0.014	13.983	−0.016	0.12+	No choice	
7	14.017	+0.018	13.986	−0.013	0.09	x	
8	14.004	+0.005	13.971	−0.028	0.10	x	
Average	14.012	+0.013	13.979	−0.020			
			Argon (Spectroscopic I.P. = 15.759 ev)				
1	15.744	−0.015	15.727	−0.032	0.10	No choice	
2	15.720	−0.039	15.704	−0.055	0.09	No choice	
3	15.723	−0.036	15.694	−0.065	0.09−	No choice	
4	15.770	+0.011	15.754	−0.005	0.11−	No choice	
Average	15.739	−0.020	15.720	−0.039			

[a] Spectroscopic ionization potentials were computed from data in *Atomic Energy Levels*, edited by Charlotte E. Moore, National Bureau of Standards Circular No. 467 (U. S. Government Printing Office, Washington, D. C., 1949) Vol. I; Vol. II, 1952; Vol. III (to be published), using the conversion factor 1 ev ↔ 12397.67(22) $\times 10^{-8}$ cm recommended by E. R. Cohen, J. W. M. DuMond, T. W. Layton, and J. S. Rollett, Revs. Modern Phys. **27**, 363 (1955).

[b] The entries in these columns reflect simply the goodness of fit of the experimental points to either a linear law or to a 1.127 power law. They are independent of the accuracy of the I.P. determinations.

tively. On the basis of this analysis, principally the accuracy of the ionization potential determinations, the data favor a linear threshold law over a 1.127 power law.

To illustrate the effect of electron energy distribution on the observed ionization curves and to demonstrate the effectiveness of the analytical procedure, experiments were performed on krypton with three different electron energy distributions. In Fig. 4, electron energy distributions A', B', and C' with half-widths 0.09 ev, 0.12 ev, and 0.17 ev, respectively, were used to calculate the corresponding curves labelled A, B, and C on the assumption that a single linear ionization process was involved. As expected, the curvature near threshold progressively increases with the width of the electron distribution. The good agreement between the experimental points and the calculated curves shows that electron distribution effects are predictable and are adequately treated by the analytical method.

Structure in the Ionization Curves

Ionization data for xenon, krypton, and argon over an extended energy range are presented in Fig. 5. For xenon the data represent the average of nine separate experiments. For krypton the data are the average of two sets of data obtained with particularly good electron energy distributions, given in Fig. 7. For argon, three sets of data were averaged. The half-widths and full widths of the electron distributions are specified on the appropriate graphs of Fig. 7.

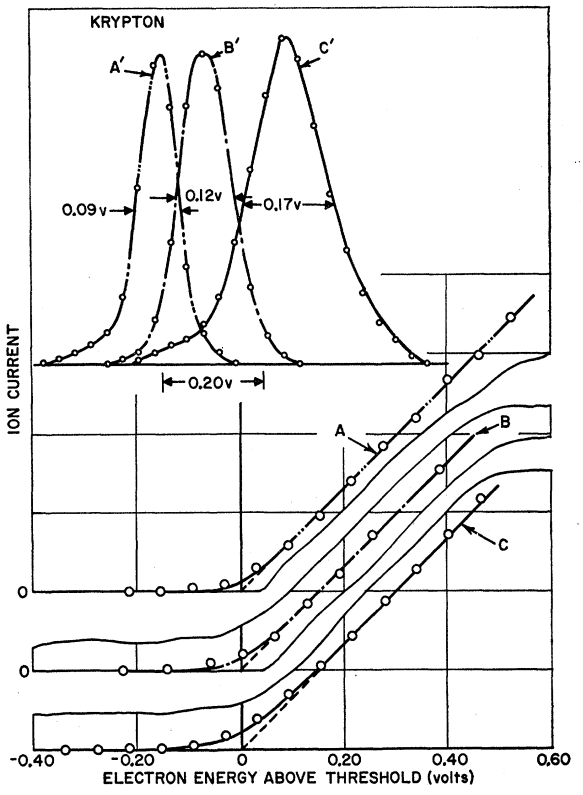

FIG. 4. Effect of electron energy distribution on observed ionization curves. Experimental points and calculated curves are given for three different distributions.

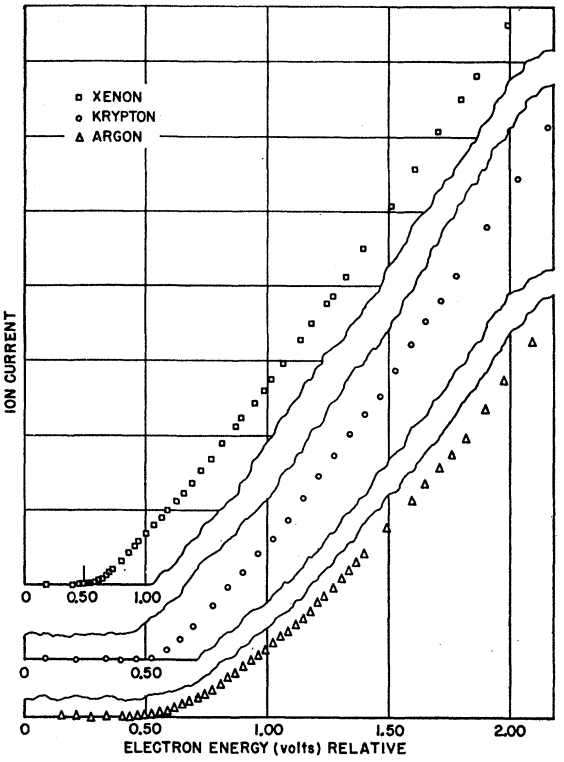

FIG. 5. Experimental data for xenon, krypton, and argon. The energy scales have been shifted and the xenon scale is compressed by a factor of two to permit the data to be displayed on a single graph.

A casual examination of the curves in Fig. 5 does not reveal the complex structure present in the ionization cross sections. It is obvious, however, that the argon curve is considerably more complicated than either the xenon or the krypton curve. Since the analysis of the data near threshold indicated that the threshold ionization process followed a linear law, it was decided to analyze the data by assuming that the ionization curve could be resolved into a number of linear ionization processes. This is consistent with the treatments of Fox *et al.*[5,10] in which they observed linear onsets at the various energy states of the ion.

Comparison with Spectral Intensity Rules

In the following treatment the ionization data are assumed to result from linear processes having onsets at the known energies of the $^2P_{\frac{3}{2}}$ and $^2P_{\frac{1}{2}}$ ground states of the corresponding ions. If ionization followed the usual spectral intensity rules, then the probability for the $^2P_{\frac{1}{2}}$ process should be $\frac{1}{2}$ that for the $^2P_{\frac{3}{2}}$ process. The results are shown in Fig. 6. The xenon data do not

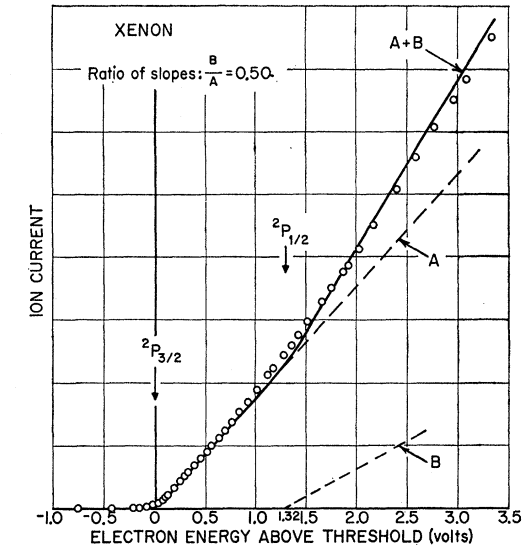

(a)

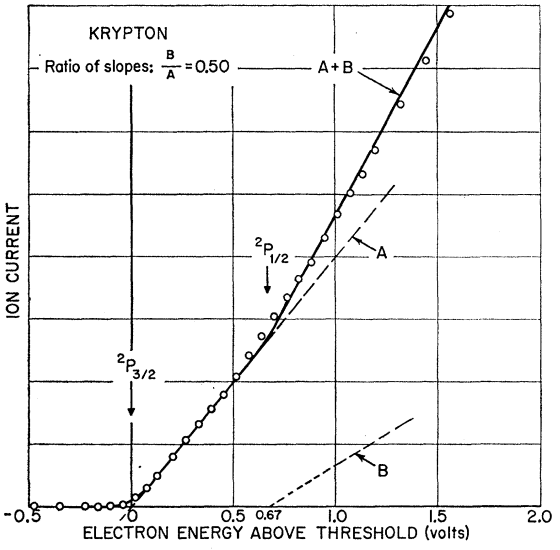

(b)

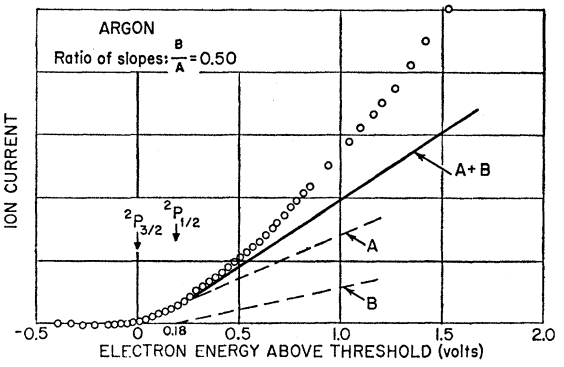

(c)

FIG. 6. Attempt to fit the ionization data for xenon, krypton, and argon with onsets at the $^2P_{\frac{3}{2}}$ and $^2P_{\frac{1}{2}}$ states according to the usual spectral intensity rules. The statistical weights are in the ratio 2:1, resulting in a slope ratio $B/A=0.50$. The calculated curves exhibit rounding at the onsets appropriate to the electron energy distributions.

closely follow the spectral intensity rules. Excess ionization begins below the energy of the $^2P_{\frac{1}{2}}$ state; and relative to the initial process, the sum of the remaining probabilities is slightly less than $\frac{1}{2}$. The fit of the krypton data is similar to that of xenon. In the case of argon, the data cannot be even approximately described by processes at only the $^2P_{\frac{3}{2}}$ and $^2P_{\frac{1}{2}}$ states. Additional ionization effects are obviously taking place above the energy of the $^2P_{\frac{1}{2}}$ state.

Fitting Data with Linear Ionization Processes

In this analysis, the ionization curves are resolved into a series of linear ionization processes, without restricting onsets to known spectroscopic states. The curves are normalized so that the initial linear process has unity slope. Threshold curvature due to the electron energy distribution has been included for each process. The synthetic curve constructed from the series of linear processes is then compared with the experimental points. The results are shown in Fig. 7. The following conclusions are drawn:

Xenon. The ionization can be closely described by a series of linear ionization processes. The onsets and relative slopes are given in Fig. 7(a). The energies of onset of the processes above the I.P. are not closely correlated with spectroscopic energy states.

Krypton. In krypton, the ionization can be moderately well fitted by three linear processes. The onsets above threshold are not even approximately correlated with spectroscopic energies. On detailed examination, the

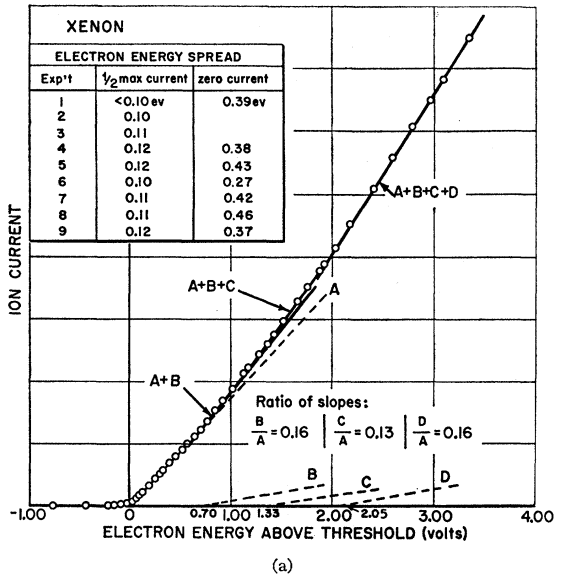

(a)

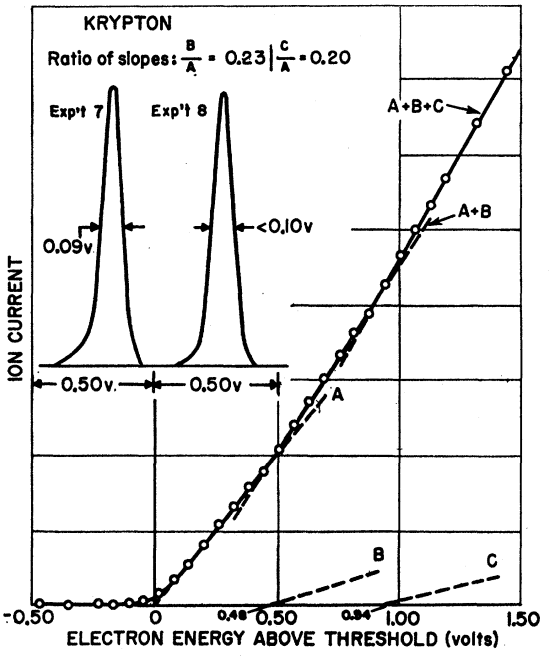

(b)

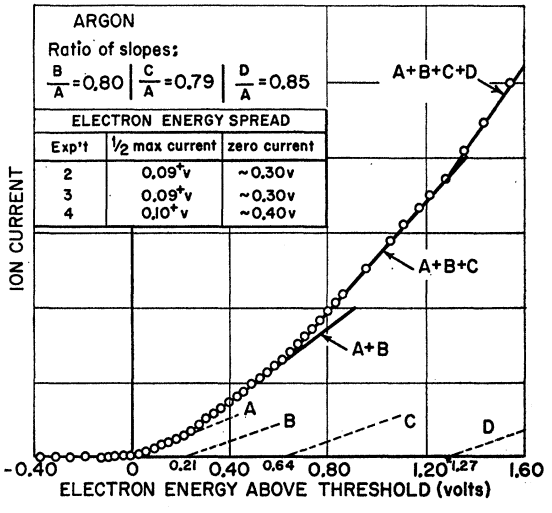

(c)

FIG. 7. Resolution of the ionization structure in xenon, krypton, and argon by a series of linear processes. Empirical fitting of the experimental data results in the onsets and slopes indicated on the graphs. The composite curves are synthetic curves constructed for these processes and include the expected roundings due to the corresponding electron energy distributions.

region between the onsets of B and C (0.48 to 0.94 v) in Fig. 7(b) is actually found not to be linear, but rather concave downward toward the energy axis.

Argon. While the ionization in argon can be accounted for by a series of linear processes, it is not clear what significance should be attached to the exact onset energies and slopes of the processes above threshold. The onset energies in Fig. 7(c), except for the I.P., are not correlated with spectroscopic energies. However, the ionization curve is closely approximated by the indicated linear processes, so that it is useful for analytical purposes and for comparison with the results of other experimenters (to be discussed later).

Possible Instrumental Sources of Error

Because mass analysis of the ions was not carried out in this apparatus, the possibility that some of the ion current could have been due to impurities must be considered. The gases were reagent grade in sealed Pyrex flasks and were introduced by an all glass sampling system to minimize impurities. Furthermore,

the studies were limited to the rare gases with relatively low I.P.'s and relatively large ionization cross sections. By operating the ion chamber at moderately high pressures ($\sim 10^{-4}$ mm Hg), considerable discrimination was obtained against background contaminants. The ionization curve shapes were not dependent on the pressure in the ion chamber and, therefore, exclude multiple collision processes from consideration. Experiments were carried out over an extended period of time, with different sample flasks, and over a range of pressures, without observing any systematic changes in the structures of the ionization curves. As a result, it is concluded that the structures in the curves are, in fact, those of the atoms being studied.

The effects of electron intensity, selection of electrons from a different region of the tungsten filament, residual magnetic fields, and ion chamber temperature were checked without observing any changes in the structures of the ionization curves.

V. DISCUSSION

Structure in the ionization cross sections cannot be explained simply by assuming linear ionization processes at only the $^2P_{\frac{3}{2}}$ and $^2P_{\frac{1}{2}}$ states of the ion. It is difficult to find a satisfactory explanation for the onsets observed in these experiments. The explanation previously suggested[5] that auto-ionization (pre-ionization) is the mechanism responsible for the structure in the rare gas ionization cross sections may eventually turn out to be correct. However, if the spectroscopic rule for occurrence of auto-ionization effects holds also in electron impact, i.e., if the magnitude of the effect is greatest near the lower continuum limit ($^2P_{\frac{3}{2}}$ state) and decreases with increase in energy, the effect of auto-ionization should be greatest 0.32 v above threshold in xenon, 0.10 v above in krypton, and 0.03 v above in argon.[25] There is no correlation in this work with such energies. Furthermore, no additional structure should be observed above the energy of the $^2P_{\frac{1}{2}}$ state; yet in each of the gases such structure is observed. From these considerations, it does not appear likely that auto-ionization will be able to account for all the structure observed in these experiments.

Comparison of Various "High-Resolution" Data

A comparison has been made of the "high-resolution" data reported by various investigators on the structures in the ionization efficiency curves of the rare gases. In principle, all ionization curves for a particular gas, after making a suitable ion current scale factor adjustment for each curve, should be superposable within the estimated experimental errors. Since all the workers in the field have presented their data as a series of linear processes, with deviation from linearity treated as an exceptional case, we have for comparison also resolved our data into a series of linear ionization processes. The procedure which we have used to compare results is to normalize the initial linear slope for each case to unity, and then for all succeeding processes measure the onset energy and the slope relative to the initial slope. Onsets and relative slopes were estimated from published curves when not otherwise specified in the references quoted. The ionization potential is used as the origin of the energy scale, so that the onsets are given in volts above threshold. The results for Xe, Kr, and A are shown in Table II.

TABLE II. Structures observed in rare gas ionization data.[a]

Atom	Source of data	Onsets (Volts above threshold)	Probability (Relative to the initial process)
Xe	RPD Fox *et al.*[b]	1.27[h]	0.36[i]
	RPD Cloutier and Schiff[c]	1.31[h]	0.27[i]
	Clarke[d]	0.82[i]	0.26[i]
		1.93[i]	0.27[i]
	This work	0.70	0.16
		1.33	0.13
		2.05	0.16
Kr	RPD Frost and McDowell[e]	0.57[i]	1.5[i]
		0.90[i]	1.1[i]
	RPD Burns[f]	0.67[h]	2.4[i]
	RPD Fox *et al.*[b]	<0.30	0.72[i]
		0.80[i]	0.45[i]
	This work	0.48	0.23
		0.94	0.20
A	RPD Fox[g]	0.2±0.1[h]	1.1[i]
	This work	0.21	0.80
		0.64	0.79
		1.27	0.85

[a] For purposes of comparison all ionization processes are assumed to have a linear dependence on the energy in excess of onset, even though in krypton all workers except Burns observe a nonlinear ionization process in a region overlapping the energy level of the $^2P_{\frac{3}{2}}$ state.
[b] See reference 5.
[c] G. G. Cloutier and H. I. Schiff, J. Chem. Phys. **31**, 793 (1959).
[d] See reference 6.
[e] See reference 8.
[f] See reference 9.
[g] R. E. Fox, Westinghouse Research Laboratories Report-60-94439-4-R2, 1956 (unpublished).
[h] These values are essentially the $^2P_{\frac{3}{2}}$ energy levels.
[i] These values are estimates made here from a study of the published data of the various investigators.

Xenon

There is fair agreement between Clarke's data and this work. A particular difference is the addition of a small onset in this work at 1.33 v. The sum of the probabilities of all the succeeding processes beyond the initial process, (final slope−initial slope)/(initial slope), is about 0.53 in Clarke's mass analyzed data as compared with 0.45 in this study. The RPD data show little agreement with Clarke's or this work in that only one onset is definitely observed above threshold, i.e., the one shown at 1.27 v in the work of Fox *et al.*[4] and at 1.31 v in the work of Cloutier and Schiff.[26] Fox *et al.* obtain a relative probability for this process of about 0.36; Cloutier and Schiff obtain a value of about 0.27.

[25] H. Beutler, Z. Physik **93**, 177 (1935).

[26] G. G. Cloutier and H. I. Schiff, J. Chem. Phys. **31**, 793 (1959).

Krypton

The only data available for comparison are those obtained by several investigators using the RPD method. The results vary considerably among the investigators. Frost and McDowell describe the structure as a gradual transition from the $^2P_{\frac{3}{2}}$ state to the $^2P_{\frac{1}{2}}$ state, beginning at about 0.57 v and extending to about 0.90 v. The relative probability of the $^2P_{\frac{1}{2}}$ state ionization process is about 2.6. Burns observes no transition ionization, but does observe a process at 0.67 v (which corresponds to the $^2P_{\frac{1}{2}}$ energy), with a relative probability of about 2.4. Fox *et al.* observe a transition process beginning at less than 0.30 v above threshold and extending above the energy level of the $^2P_{\frac{1}{2}}$ state, to about 0.80 v. The relative probability of the $^2P_{\frac{1}{2}}$ state ionization process is about 1.2.

In the present study there is an onset at 0.48 v, and another at 0.94 v. Although the energies of the onsets are in fair agreement with those of Frost and McDowell, the sum of the probabilities of the two onsets is 0.43 in our study as compared to 2.6 in their results. The discrepancy of a factor of 6 in the probabilities is most disturbing.

It is clear that at best only one of these four widely divergent krypton experimental results can be correct.

Argon

In the literature, the only detailed experimental data with resolution comparable to that reported here are the RPD argon data of Fox *et al.*[4] and Fox.[27] The earlier work[4] indicated that argon ionization followed a linear law from threshold to approximately 1.5 v above threshold. This is the example most often quoted to illustrate the advantages of using nearly monoenergetic electrons in ionization studies.[28,29] However, later studies[27] showed that there was, in fact, an additional onset at 0.2 v above threshold with a relative probability of 1.1. The argon data of this paper are consistent with a series of onsets at 0.21 v, 0.64 v, and 1.27 v above threshold with relative slopes of 0.80, 0.79, and 0.85, respectively. The onsets at 0.64 v and 1.27 v above threshold have not been previously reported in the literature.

Considerable structure in the ionization efficiency curve of argon has also been noted in other studies. Fineman and Bouffard[30] recently made a survey of the results of different workers and concluded that there was evidence for a break in the argon curve at an energy 1.0 ± 0.2 v above the ionization potential.

To add to the confusion on ionization in argon, Marmet and Kerwin,[22] in testing their electrostatic electron energy analyzer with argon, abstracted the "salient features" of many runs to obtain an ionization curve consisting of two linear processes separated by almost exactly the spectroscopically known energy difference of the $^2P_{\frac{3}{2}}$ and $^2P_{\frac{1}{2}}$ states. The actual experimental data were not presented, so that the degree of fit of this simple formulation cannot be readily ascertained. Furthermore, there is the complication that at somewhat higher pressures there is an additional linear onset below the ionization potential of argon, attributed to the formation of A_2^+, but which is much larger than expected for A_2^+ ions at these pressures according to the work of Hornbeck and Molnar.[31]

Comparison of "High-Resolution" Data with Conventional "Low-Resolution" Mass Spectrometric Data

Previous workers[3,32,33] using conventional mass spectrometers with simple tungsten-filament or oxide-cathode electron sources have obtained results in good agreement for the rare gas atom ionization efficiency curves. In particular, a long tail at threshold was always observed for argon as contrasted with smaller tails for neon, krypton, and xenon.

With the advent of methods of obtaining effectively small energy spreads in electron beams, the tendency has been to treat inconsistencies between the more conventionally obtained mass spectrometric data and the newer data as being entirely due to inadequacies in the earlier experiments, e.g., thermal electron energy spreads, ion drawout fields, etc. Fundamentally there is no reason why ionization data obtained under controlled conditions on mass spectrometers with thermal electron energy spreads should not be entirely consistent with the most highly resolved data. The various "high-resolution" data compared in Table II for xenon, krypton, and argon are checked for consistency with earlier mass spectrometric data. The comparison will be made between the earlier mass spectrometric data and synthetic curves constructed from the results obtained in the various "high-resolution" studies. Although this procedure is insensitive to small deviations in the structure of ionization efficiency curves, it is a method for reducing all data to a common denominator. Any significant differences should be observable.

Several years ago, data on the ionization of rare gases were obtained at this Laboratory[33] on a modified Westinghouse Type LV mass spectrometer. To eliminate electron energy spread due to the ion drawout

[27] R. E. Fox, Westinghouse Research Laboratories Report-60-94439-4-R2, 1956 (unpublished).
[28] *Handbuch der Physik*, edited by S. Flügge (Springer-Verlag, Berlin, 1956), Vol. 36, Part II, p. 314.
[29] E. U. Condon and Hugh Odishaw, *Handbook of Physics* (McGraw-Hill Publishing Company, Inc., New York, 1958), Part 7, p. 134.
[30] M. A. Fineman and R. Bouffard, Bull. Am. Phys. Soc. **5**, 15 (1960).
[31] J. A. Hornbeck and J. P. Molnar, Phys. Rev. **84**, 621 (1951).
[32] V. H. Dibeler, F. L. Mohler, and R. M. Reese, J. Research Natl. Bur. Standards **38**, 617 (1947).
[33] S. N. Foner, paper presented at Division of Chemical Physics Symposium on Mass Spectrometry, American Physical Society, Washington, D. C., May 1952 (unpublished).

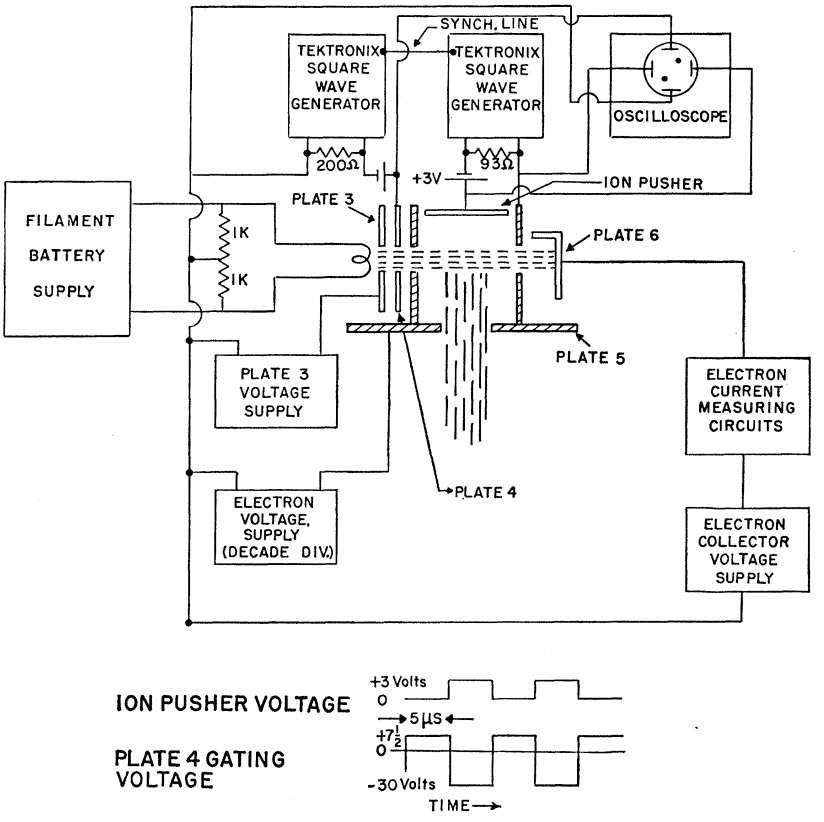

FIG. 8. Block diagram of electron voltage supply and pulsing circuits for the mass spectrometer.

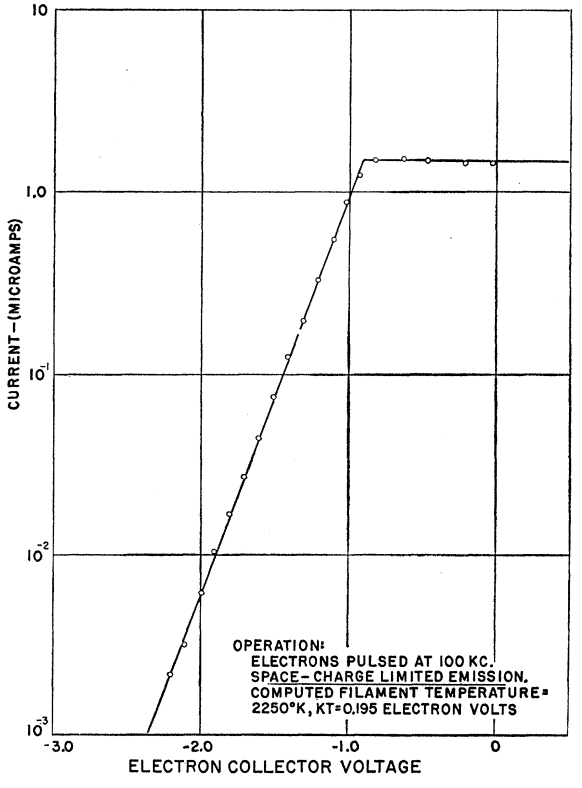

FIG. 9. Typical electron stopping potential curve.

field, the electron beam and ion pusher field were synchronously pulsed at 100 kc/sec so that ionization occurred at zero ion drawout field. A block diagram of the electron voltage supply and the associated measuring circuits is shown in Fig. 8. The electron energy distribution was determined by stopping-potential measurements. By operating the electron gun space-charge-limited to reduce field effects and eliminate filament reflection coefficient effects, it was found that the electron energy distribution was closely Maxwellian as shown by the stopping-potential curve in Fig. 9.

The ion current $I(V)$ corresponding to a Maxwell-Boltzmann electron distribution is

$$I(V)=\frac{1}{(kT)^2}\int_V^\infty (E-V)e^{[-(E-V)/kT]}P(E)dE, \quad (5)$$

where V is the electron accelerating potential, k is the Boltzmann constant, T is the absolute temperature of the filament, and $P(E)$ is proportional to the ionization cross section for electrons of energy E. The ionization probability function $P(E)$ in this study will be assumed to be known from the "high-resolution" experiments. Integration of Eq. (5) is carried out directly for a linear ionization probability function and can be carried out numerically for any arbitrary $P(E)$ function. The resulting synthetic curve is then normalized and superposed on the experimental mass spectrometric data.

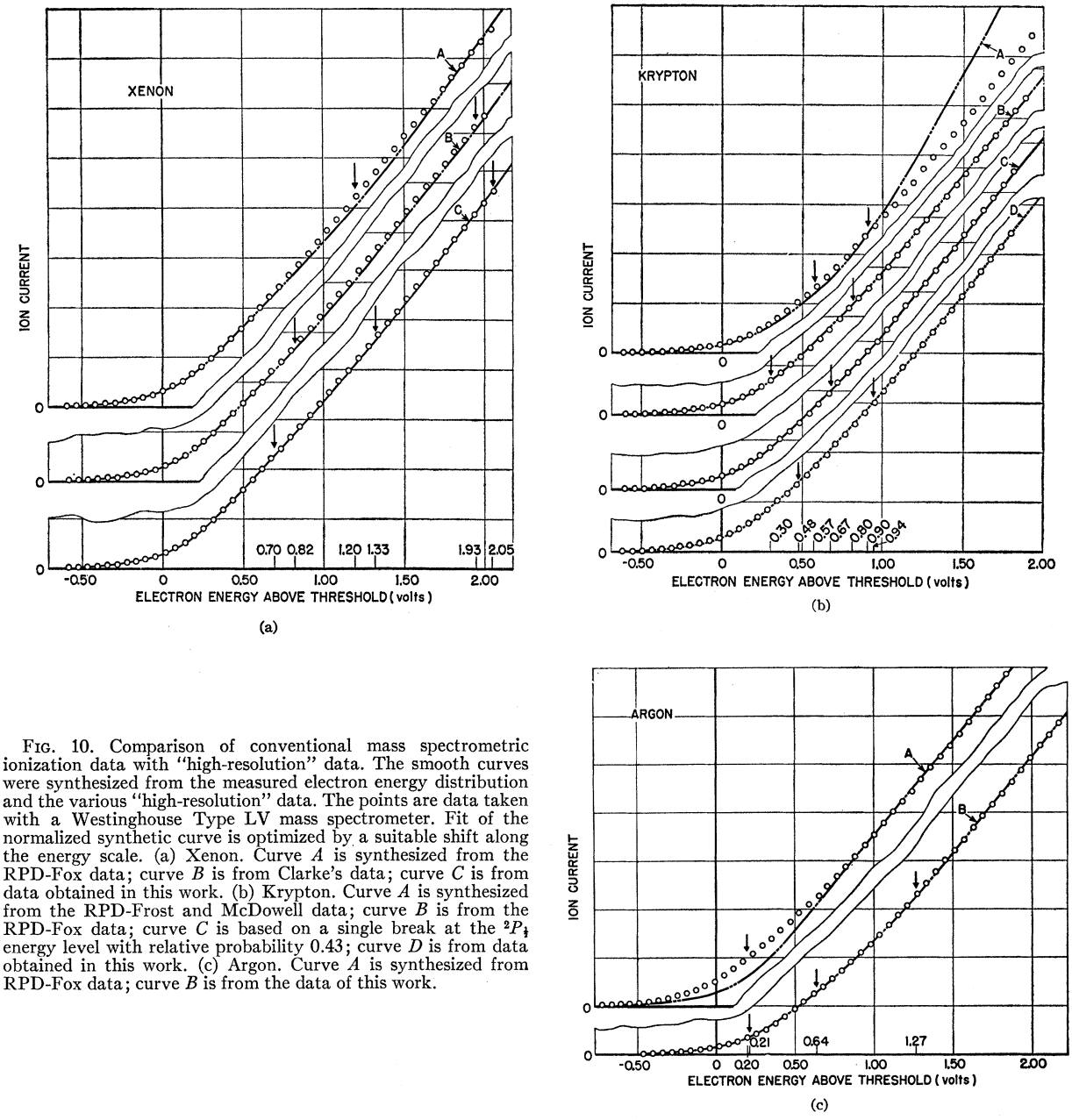

FIG. 10. Comparison of conventional mass spectrometric ionization data with "high-resolution" data. The smooth curves were synthesized from the measured electron energy distribution and the various "high-resolution" data. The points are data taken with a Westinghouse Type LV mass spectrometer. Fit of the normalized synthetic curve is optimized by a suitable shift along the energy scale. (a) Xenon. Curve A is synthesized from the RPD-Fox data; curve B is from Clarke's data; curve C is from data obtained in this work. (b) Krypton. Curve A is synthesized from the RPD-Frost and McDowell data; curve B is from the RPD-Fox data; curve C is based on a single break at the $^2P_{\frac{1}{2}}$ energy level with relative probability 0.43; curve D is from data obtained in this work. (c) Argon. Curve A is synthesized from RPD-Fox data; curve B is from the data of this work.

Xenon. The results are shown in Fig. 10(a). It will be noted that the experimental data did not extend to sufficiently high energies for a test of fit to final onsets in the synthetic curves B based on data of Clarke[6] and C on data of this work. However, these curves, within the region covered, give a better fit to the experimental data than does curve A which is calculated from the structure reported in the RPD data.[5] The prominent break at the $^2P_{\frac{1}{2}}$ energy level observed in the RPD experiment produces an undershoot in the curve at about 1.3 volts above threshold which should have been observed in the earlier mass spectrometric data.

Krypton. The results are shown in Fig. 10(b) and are summarized as follows: There are three curves which equally well fit the experimental data. They are curve B, based on results of Fox *et al.*[5]; curve C, based on a single break at the $^2P_{\frac{1}{2}}$ energy level with a relative slope of 0.43; and curve D, based on data obtained in this work. Curves B, C, and D represent deviations in structure to which the experimental data are insensitive, i.e., this test gives no conclusions as to whether 1 or 2 breaks exist in the krypton ionization efficiency curve. It is obvious that curve A, based on the data of Frost and McDowell,[8] does not fit the experimental data. There-

fore, in krypton, only the results of Frost and McDowell and those of Burns[9] which are similar (see Table II) are considered irreconcilable with earlier mass spectrometric data.

Argon. The results are shown in Fig. 10(c). It is seen that curve *A* calculated from RPD data[27] cannot fit the experimental data; the disagreement is marked. It is equally clear that the curve *B* based on the data of this work is a very good fit to the mass spectrometric data.

VI. CONCLUSIONS

The ionization efficiency curves for xenon, krypton, and argon obtained in this study with an electron energy analyzer are in excellent agreement with the lower-resolution results obtained with a conventional mass spectrometer operated under carefully controlled conditions. Although this agreement is not sensitive to small variations in the structure of the ionization efficiency curves, it effectively eliminates the possibility of gross inconsistencies in structure.

The unsatisfactory state of agreement between the various published "high-resolution" results on ionization in the rare gases is clearly revealed by the tabulation of onset energies and slopes in Table II. There is considerable disparity in the onset energies, and even more disagreement in the relative probabilities of the various ionization processes. Some of the data obtained by the RPD method are irreconcilable with the lower resolution mass spectrometric data.

Except for the threshold ionization process, for which there is good evidence that this is a linear process, the resolution of structure at higher energies as a series of linear processes is subject to some uncertainty and it is not clear what significance should be attached to the exact onset energies and the slopes of the processes above threshold. The problem is compounded by the fact that the onset energies are generally not correlated with spectroscopic energy states. The theory for ionization to excited states, unfortunately, has not been sufficiently developed to be applied to the interpretation of the structures in ionization curves. For analytical purposes, fitting the data with a series of linear ionization processes is consistent with previous treatments of the subject, closely approximates the ionization curves, and provides a convenient means for comparing the results of various investigators. It is difficult to account for the structure in the ionization curves by auto-ionization and no alternative explanation is offered.

In this paper we have used a rather simple experimental approach to avoid sources of error which may be present in more complicated instruments. The ionization for Xe, Kr, and A obtained by extrapolating according to a linear threshold law agree with spectroscopic values to within the experimental error (0.02 ev). The experimental difficulties in obtaining data even for xenon with its relatively large ionization cross section and low ionization potential, and the limitations set by the absence of mass analysis in the apparatus, suggest that while a few more atoms or molecules could be studied, further efforts probably will require improvements in electron density and the incorporation of a mass analyzer.